

# A HIGH-FREQUENCY BEM FOR 3D ACOUSTIC SCATTERING

Jonathan A. Hargreaves and Yiu W. Lam

Acoustics Research Centre, University of Salford, Salford, M5 4WT, UK e-mail: j.a.hargreaves@salford.ac.uk

## Stephen Langdon

Department of Mathematics and Statistics, University of Reading, Reading RG6 6AX, UK

#### David P. Hewett

Mathematical Institute, University of Oxford, Oxford, OX2 6GG, UK

The Boundary Element Method (BEM) is a powerful method for simulating scattering of acoustic waves which has many advantages, particularly when the problem concerns an object in an unbounded medium. Its applications are however limited in practice because standard schemes have a computational cost which grows extremely quickly as size and frequency is increased. Fundamentally this occurs because the number of degrees of freedom N required to discretise the boundary with elements that are small with respect to wavelength increases with frequency, scaling  $O(f^2)$  in 3D or O(f) in 2D. BEM produces dense matrices relating these elements, resulting in  $O(N^2)$  computation and storage costs, so  $O(f^4)$  in 3D or  $O(f^2)$  in 2D. Accelerated BEM algorithms such as the Fast Multipole Method can reduce this dependency on N to O(N) for small f and  $O(N \log N)$  for larger f, but the trend of increasing cost with frequency due to the scaling of N with f remains. An alternative strategy toward remedying this is to design discretisation schemes which do not require more degrees of freedom at higher frequencies. This is the approach adopted by the so called 'High frequency BEM' (HF-BEM) algorithms, such as Partition-of-Unity BEM (PU-BEM) and Hybrid Numerical Asymptotic BEM (HNA-BEM). These typically represent the pressure on the boundary using basis functions which are products of suitably chosen oscillatory functions, multiplied with standard piecewise-polynomial interpolators defined on a coarse, frequencyindependent mesh. Such approaches have been shown to achieve significant savings, for example reducing the number of degrees of freedom required to  $O(\log f)$  for polygonal obstacles in 2D. This paper will give an overview of these methods and will demonstrate a new HNA-BEM algorithm for the modelling of rectangular plates in 3D.

### 1. Introduction

In numerical schemes for solving wave scattering problems it is commonplace to approximate the solution on the surface of the obstacle as a weighted sum of basis functions which are chosen to

be piecewise polynomials. This approach is effective and widely applied, however suffers from the restriction that the number of degrees of freedom required to represent the oscillating solution must grow at least linearly in each direction as frequency increases in order to maintain accuracy. Thus a standard Boundary Element Method (BEM) for a 3D scattering problem, reduced to an integral equation on the 2D surface bounding the scattering domain, would require at least quadratic growth in the number of degrees of freedom with frequency. Various schemes exist for solving the resulting system of simultaneous equations; however the computation and storage costs of these must at least grow with this trend.

To mitigate this, there has been much recent interest in the development of 'high-frequency' BEM algorithms. These attempt to give improved performance at high frequencies by choosing basis functions which have the oscillatory behaviour similar to that which the solution is expected to possess; a common choice is plane waves with the same wavelength as the acoustic waves in the medium, multiplied by standard piecewise polynomial functions defined on a coarse mesh which is independent of frequency. The intention here is that the plane waves will efficiently represent the (often largely predictable) oscillation in the surface quantities, leaving the polynomial functions to interpolate the envelope of these oscillations, a quantity which should be slowly varying with respect to wavelength. The question then becomes how to choose the number of these plane waves and the directions in which they propagate, and two dominant strategies exist for this.

A straightforward strategy would be to choose the plane wave directions to be uniformly spaced in angle; this is what is adopted in the Partition-of-Unity BEM¹ (PU-BEM). The result of this is an algorithm which can be readily applied and which can achieve engineering accuracy of around 1% error with 2-3 degrees of freedom per wavelength, a significant saving compared the 8-10 degrees of freedom per wavelength required to achieve this accuracy with standard piecewise polynomial based schemes. However this is only a fixed saving and the cost with respect to frequency still scales the same as standard BEM.

An alternative strategy is to choose the plane wave directions to match leading-order behaviour known to be dominant in the high frequency (asymptotic) solution. This is the approach used in the Hybrid-Numerical-Asymptotic BEM<sup>2</sup> (HNA-BEM), so called because the asymptotic behaviour has been incorporated into the numerical approximation space (i.e. the set of basis functions), thus the algorithm is a hybrid of these two approaches. This has been proven to be extremely efficient for obstacle geometries where the asymptotic behaviour is known, and can break the dependency of N on S0 of reading convex polygonal obstacles may be accurately modelled in 2D using only S10 degrees of freedom<sup>3</sup>, a significant saving compared to the S10 requirement by standard methods. To date however, the requirement that the asymptotic behaviour is well understood has restricted these ideas mostly to 2D scattering problems (one notable exception being Ref. 4 where the problem of scattering by smooth convex 3D obstacles was considered).

Here, we describe a HNA-BEM algorithm for the problem of scattering by a planar rectangular screen in 3D. The equivalent 2D problem was studied in Ref. 5, where a complete numerical analysis proved that accuracy could be maintained with N growing as  $O(\log f)$  and numerical results suggested that accuracy could be maintained with no growth in N at all. Due to the added complexity induced by multiple redirections from the edges and corners of the screen in 3D, the extension of these ideas to 3D is highly nontrivial. We are though able to demonstrate, via numerical results, that by incorporating some of the oscillatory behaviour away from the edges of the screen into our approximation space, we can achieve reasonable accuracy for a range of frequencies using only a small number of degrees of freedom, this number crucially independent of frequency.

#### 2. Problem Statement

We consider the 3D problem of scattering of the time harmonic incident plane wave  $P_i(\mathbf{x}) = e^{ik\mathbf{x}\cdot\mathbf{d}_i}$ , where  $k = 2\pi f/c > 0$  is the wavenumber,  $\mathbf{x}$  is a point in 3D Cartesian space and  $\mathbf{d}_i$  is a

unit direction vector, by a sound soft planar screen. This is denoted by  $\Gamma$  and is chosen to lie in the z=0 plane with normal vector  $\hat{\mathbf{n}} = \hat{\mathbf{z}}$  and to be square, with all sides of length  $2\pi$  meters.

The boundary value problem (BVP) we wish to solve is: given the incident pressure field  $P_t(\mathbf{x})$ , determine the total pressure field  $P_t(\mathbf{x})$  such that  $\nabla^2 P_t(\mathbf{x}) + k^2 P_t(\mathbf{x}) = 0$  for  $\mathbf{x} \notin \Gamma$  and  $P_t(\mathbf{x}) = 0$  for  $\mathbf{x} \in \Gamma$ , and that the scattered pressure  $P_s = P_t - P_i$  satisfies the Sommerfeld radiation condition. The solution  $P_t(\mathbf{x})$  may be expressed as a boundary integral over  $\Gamma$ :

(1) 
$$P_t(\mathbf{x}) = P_i(\mathbf{x}) - \iint_S G(\mathbf{x}, \mathbf{y}) \phi(\mathbf{y}) d\mathbf{y}.$$

Here  $G(\mathbf{x}, \mathbf{y}) = e^{ikR}/4\pi R$ , where  $R = |\mathbf{x} - \mathbf{y}|$ , is the free-space Green's function. It can be shown that the unknown surface quantity  $\phi(\mathbf{y})$  corresponds physically to the jump in the surface normal derivative of  $P_t$  (i.e. in  $\partial P_t/\partial n = \hat{\mathbf{n}} \cdot \nabla P_t$ ) from one side of the screen to the other. Taking  $\mathbf{x}$  to lie on the screen and using the boundary condition  $P_t(\mathbf{x}) = 0$  for  $\mathbf{x} \in \Gamma$  allows  $\phi(\mathbf{y})$  to be found by solving the boundary integral equation (see e.g. Ref. 2 Section 7.6):

(2) 
$$P_i(\mathbf{x}) = \mathcal{S}_k\{\phi\}(\mathbf{x}) = \iint_{S} G(\mathbf{x}, \mathbf{y})\phi(\mathbf{y})d\mathbf{y}, \quad \mathbf{x} \in \Gamma.$$

#### 2.1 Equivalence with an aperture in a rigid screen

We acknowledge that the BVP we have chosen to solve is one without a clear physical manifestation in acoustics; a thin plate which is rigid is a common occurrence but a thin obstacle with a pressure-release boundary condition is not. We have chosen to initially address this problem primarily because it allows more flexible choices of discretisation scheme compared to the rigid plate, where the requirement for  $C^{1,\alpha}$  continuity in the solution<sup>6</sup> (arising from the use of a hyper-singular integral operator) places additional restrictions on the basis functions.

We would however like to emphasise that the chosen problem is equivalent to a problem which is realisable in acoustics following Babinet's principle. This is the problem of an aperture in an infinite rigid planar screen (sometimes called a 'breakwater' problem); it is analysed in detail in Ref. 5. Two equivalent cases are depicted in Fig. 1 (note these are shown for illustrative purposes and are actually computed using the 2D screen algorithm described in Ref. 5, not the algorithm described herein). Specifically, if  $P_r$  is the reflection of  $P_i$  in the infinite rigid planar screen (without the aperture), then the total pressure  $P_t'$  in the aperture problem in Fig. 1b is  $P_t' = P_i + P_r - P_s$  for  $\mathbf{x}$  above the screen, and  $P_t' = -P_s$  for  $\mathbf{x}$  below the screen. Hence the results for the equivalent aperture problem may be easily calculated by an additional step with a cost which is independent of frequency.

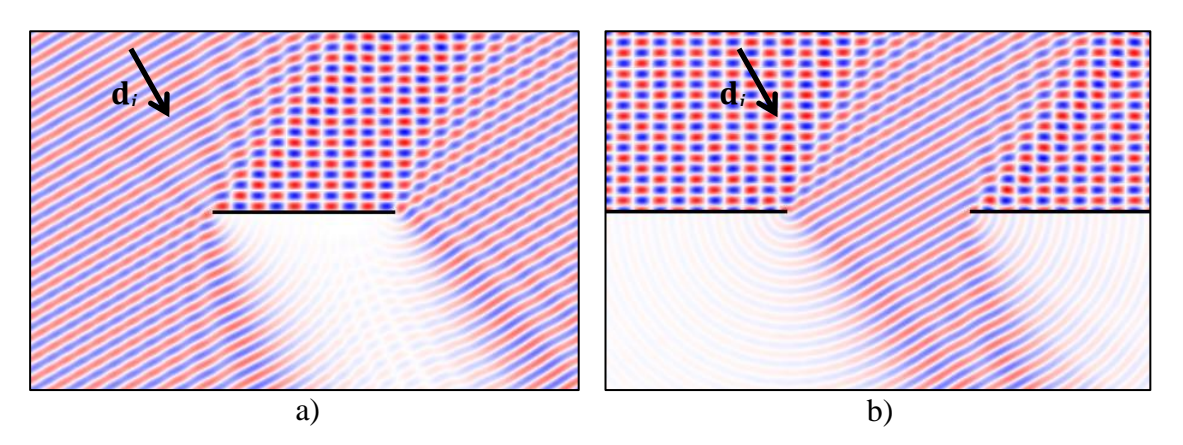


Figure 1: Total pressure  $P_t$ , with k = 10 and  $d_i$  as indicated, for the equivalent problems of: a) a sound soft screen; b) an aperture in an infinite rigid screen.

#### 3. HNA-BEM scheme

#### 3.1 Approximation Space

The key idea of our approach is to construct a bespoke approximation space with which to numerically solve Eq. 2. In particular we wish to incorporate into it the known high frequency asymptotic behaviour of the solution. Specifically, we express  $\phi(y)$  for  $y \in \Gamma$  as:

(3) 
$$\phi(\mathbf{y}) = \phi_{KA}(\mathbf{y}) + \psi(\mathbf{y}).$$

Here  $\phi_{KA}(\mathbf{y}) = -2 \operatorname{sign}(\mathbf{\hat{n}} \cdot \mathbf{d}_i) \partial P_i / \partial n(\mathbf{y})$  is the Kirchhoff approximation to the jump in  $\partial P_t / \partial n$  across the screen (i.e. the value  $\varphi$  would take if the screen filled the entire plane z = 0). This has been deliberately separated since it gives the complete solution as  $k \to \infty$ . It follows that the residual quantity  $\psi(\mathbf{y})$  will become less significant as k increases, and it is this that we will approximate numerically.

It is well known that the jump in  $\partial P_t/\partial n$  across a sound-soft screen contains a  $1/\sqrt{d}$  singularity, where d is the shortest distance from a point on the screen to a point on its edge. An efficient (non HNA-BEM) integral equation method for scattering by screens has recently been proposed which builds this behaviour into its boundary integral operators, however we will address the edge singularities by using a graded mesh of standard piecewise polynomial elements to approximate  $\psi(\mathbf{y})$  within one tenth of a wavelength of the edge of the screen. Despite a standard approximation scheme being used here, the number of degrees of freedom it contains scales just O(f) since the width of this mesh (perpendicular to the edge) is inversely proportional to frequency.

Away from the edges of the screen we approximate  $\psi(\mathbf{y})$  by a weighted sum of oscillatory functions multiplied by piecewise polynomial functions  $V_n(\mathbf{y})$ , which are defined on a coarse mesh of nine elements which are large with respect to wavelength (see Fig. 2). As discussed in section 1, we will choose our oscillatory functions to be plane waves propagating in predefined directions specified by unit vectors  $\mathbf{d}_m$ . The entire statement for  $\psi$  is as follows, where  $\psi_N$  is the numerical approximation to  $\psi$  and  $w_{m,n}$  are the unknown scalar weights:

(4) 
$$\psi(\mathbf{y}) \approx \psi_N(\mathbf{y}) = \sum_{m=1}^M e^{\mathrm{i}k\mathbf{y}\cdot\mathbf{d}_m} \sum_{n=1}^N w_{m,n} V_n(\mathbf{y}).$$

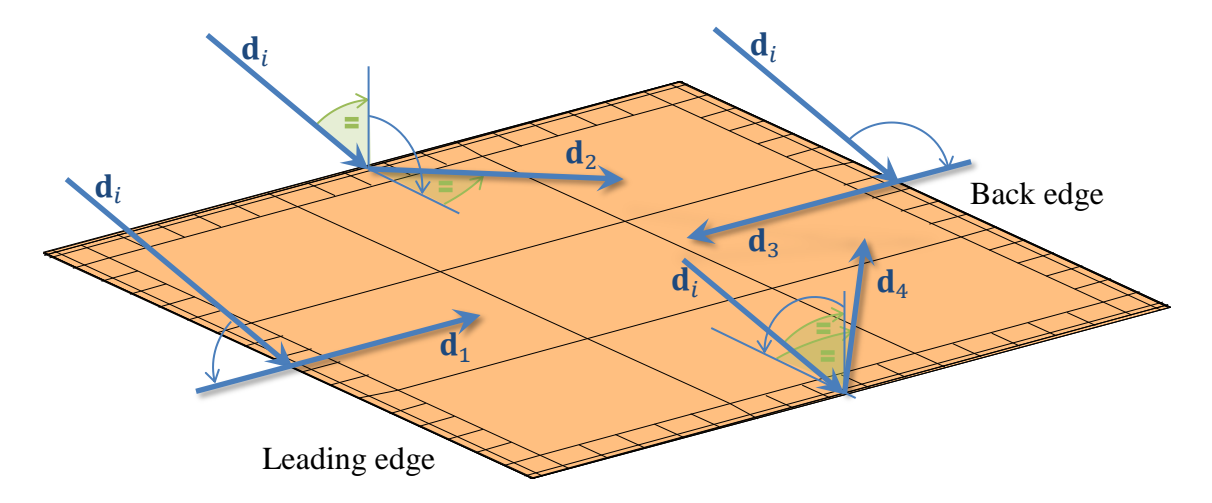


Figure 2: Discretisation scheme on the screen, showing the incident wave direction  $(d_i)$ , the leading order diffraction directions on the screen  $(d_1, d_2, d_3, d_4)$ , the graded mesh of standard elements around the rim of the plate and the coarse mesh of hybrid elements in the middle

The goal is to choose set of direction vectors  $\mathbf{d}_m$  in such a way that the envelope which the piecewise polynomial functions  $V_n$  are required to interpolate is (relatively) non-oscillatory. For the equivalent 2D problem (see Ref. 7) it is sufficient to take M=2, in which the two corresponding envelope functions are provably non-oscillatory (i.e. all of the oscillations are captured completely by two phase functions). For the 3D problem this is not the case, since the waves directed by the edges and corners of the screen are re-reflected infinitely often by the other edges and corners of the screen, taking a different direction of travel after each redirection. However, it turns out that with a judicious choice of  $\mathbf{d}_m$  in Eq. 4 we can represent  $\psi(\mathbf{y})$  to a reasonable degree of accuracy (away from the edges of the screen where the solution is singular) using only a small value of N. Specifically, we choose M=4, and  $\mathbf{d}_m$  to be the directions of the first-order diffracted rays predicted by the Geometrical Theory of Diffraction (see Ref. 5 section 7.6 for details, also depicted graphically in Fig. 2 herein), with one such wave associated with each of the four edges of the screen. Numerical results in section 7.6 of Ref. 5 (in which a number of candidate phase functions were used in a "best fit" approximation to a reference result for  $\phi$ ) suggest that this choice offers a good balance between accuracy and efficiency.

#### 3.2 Galerkin Scheme

We use a Galerkin approach to compute a discrete version of Eq. 2. This requires additional numerical integration but is more appropriate for oscillatory basis functions since they have no inherent zeroes at which to place collocation points. Defining  $b_{m,n}(\mathbf{y}) = e^{\mathrm{i}k\mathbf{y}\cdot\mathbf{d}_m}V_n(\mathbf{y})$ , we seek to find the weights  $w_{m,n}$  such that the following holds for all m' from 1 to M and all n' from 1 to N:

$$\langle \mathcal{S}_k \{ \psi_N \}, b_{m',n'} \rangle_{\Gamma} = \langle P_i - \mathcal{S}_k \{ \phi_{KA} \}, b_{m',n'} \rangle_{\Gamma}$$

Here the angled brackets denote an  $L^2$  inner product computed over  $\Gamma$ . Use of this leads to our piecewise polynomial functions being chosen to be tensor products of scaled Legendre polynomials in x and y, since these are orthogonal with respect to this norm.

#### 4. Numerical Results

We now present numerical results for the solution of Eq. 4 with  $\mathbf{d}_i = (1/\sqrt{2}, 0, 1/\sqrt{2})$ . We investigate this using piecewise polynomials with maximum order p = 0, 1, 2, giving 1, 4, 9 polynomials respectively on each coarse element, and four plane wave directions. For p = 0 we have 4 degrees of freedom per coarse element, rising to 16 degrees of freedom per coarse element for p = 1 and 36 degrees of freedom per coarse element for p = 2. With nine coarse elements altogether, we then have, for p = 0, 1, 2, respectively 36, 144, and 324 total degrees of freedom on the central part of the screen (i.e. the whole screen except for the band within a tenth of a wavelength of the edge), and we keep these values unchanged for the different values of k tested. Note that this central part of the screen covers k = 0.2 wavelengths in each direction, so a standard scheme requiring, say, 10 degrees of freedom per wavelength, might require of the order of  $100(k - 0.2)^2$  degrees of freedom on this region in order to represent the solution to "engineering accuracy". In Fig. 3 we plot on a logarithmic scale the relative  $L^2$  error in  $\varphi$  on this central section, versus k, for p = 0, 1, 2, demonstrating that we can achieve a reasonable level of accuracy using this approach with a very small number of degrees of freedom compared to standard methods.

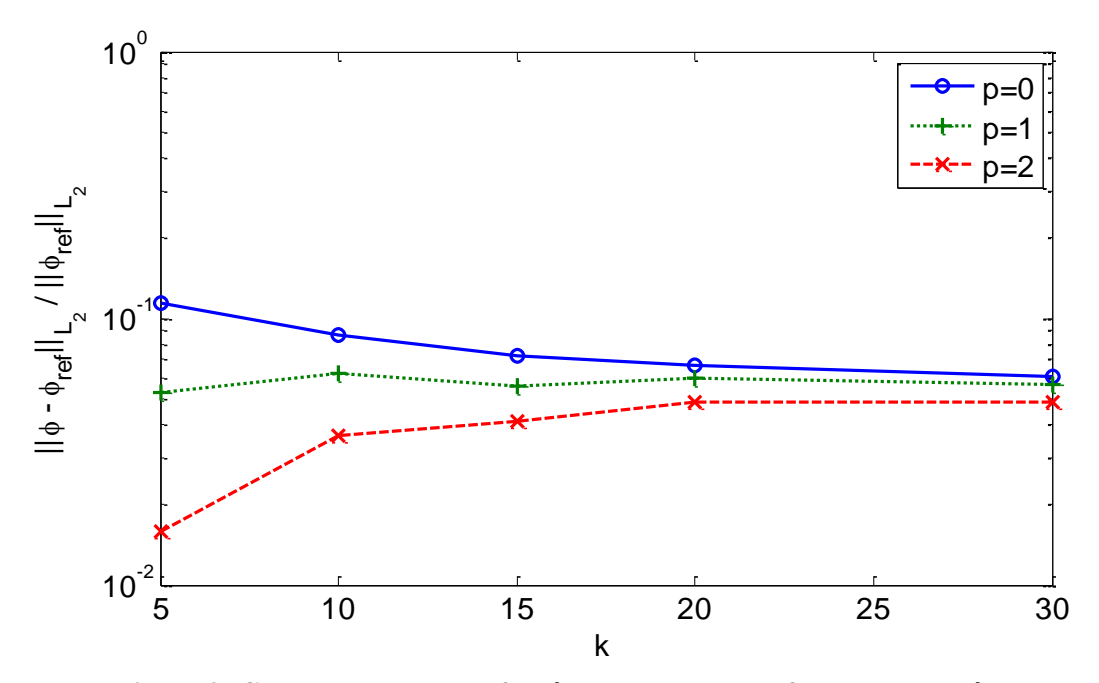


Figure 3: Convergence results for  $\phi$  compared to a reference result  $\phi_{\rm ref}$ . Vertical axis is the  $L^2$  norm of the error  $\phi - \phi_{\rm ref}$  normalised by the  $L^2$  norm of  $\phi_{\rm ref}$ .

# 5. Conclusions

A Hybrid-Numerical-Asymptotic Boundary Element Method scheme has been presented for the problem of computing acoustic scattering from a sound soft screen. This utilised a coarse mesh of hybrid elements in the middle of the screen, with a number of degrees of freedom which is independent of frequency, and a narrow graded mesh around the edge of the screen, for which the number of degrees of freedom scales linearly with frequency. Error on the centre section was seen to be reasonably small and fairly independent of frequency, despite using a very small number of degrees of freedom compared to standard methods.

# 6. Acknowledgements

This work was supported by the UK Engineering and Physical Sciences Research Council [grant number EP/J022071/1 "Enhanced Acoustic Modelling for Auralisation using Hybrid Boundary Integral Methods"].

### **REFERENCES**

- 1 Perrey-Debain, E., Laghrouche O., Bettess P. and Trevelyan J. Plane-wave basis finite elements and boundary elements for three-dimensional wave scattering, *Philosophical transactions*. Series A, Mathematical, physical, and engineering sciences, **362**, 561–577, (2004)
- 2 Chandler-Wilde S. N., Graham I. G., Langdon S. and Spence E. A. Numerical-asymptotic boundary integral methods in high-frequency acoustic scattering, *Acta Numerica*, **21**, 89-305 (2012).
- 3 Langdon S. and Chandler-Wilde S. N. A Galerkin boundary element method for high frequency scattering by convex polygons, *SIAM Journal on Numerical Analysis*, **45** (2), 610–640. (2007)
- 4 Ganesh M. and Hawkins S. C. A Fully Discrete Galerkin Method for High Frequency Exterior Acoustic Scattering in Three Dimensions, *Journal of Computational Physics*, **230**, 104-125 (2011).
- 5 Chandler-Wilde, S. N., Hewett D. P. and Langdon S. A frequency-independent boundary element method for scattering by two-dimensional screens and apertures, *IMA Journal of Numerical Analysis*, published online at doi:10.1093/imanum/dru043 (2014).
- 6 Krishnasamy G., Schmerr L. W., Rudolphi T. J. and Rizzo F. J. Hypersingular Boundary Integral Equations: Some Applications in Acoustic and Elastic Wave Scattering, *Journal of Applied Mechanics*, **57** (2), 404-414 (1990).
- 7 Bruno O. P. and Lintner S. K. A high-order integral solver for scalar problems of di raction by screens and apertures in three-dimensional space, *Journal of Computational Physics*, **252**, 250-274, (2013).